Front. Phys., 2012, 7(2): 193–199
DOI 10.1007/s11467-011-0217-9

REVIEW ARTICLE

Superconductivity of topological matters induced via pressure

Jun-liang Zhang[1,2], **Si-jia Zhang**[1], **Hong-ming Weng**[1], **Wei Zhang**[1], **Liu-xiang Yang**[1], **Qing-qing Liu**[1], **Pan-pan Kong**[1], **Jie Zhu**[1], **Shao-min Feng**[1], **Xian-cheng Wang**[1], **Ri-cheng Yu**[1], **Lie-zhao Cao**[2], **Shoucheng Zhang**[3], **Xi Dai**[1], **Zhong Fang**[1], **Chang-qing Jin**[1,†]

[1] *Beijing National Laboratory for Condensed Matter Physics & Institute of Physics, Chinese Academy of Sciences, Beijing 100190, China*

[2] *Department of Physics, University of Science & Technology of China, Hefei 230026, China*

[3] *Department of Physics, McCullough Building, Stanford University, Stanford, CA 94305-4045, USA & Center for Advanced Study, Tsinghua University, Beijing 100084, China*

E-mail: [†] *Jin@iphy.ac.cn*

Received October 9, 2011; accepted November 20, 2011

By applying pressure on the topological insulator Bi_2Te_3 single crystal, superconducting phase was found without a crystal structure phase transition. The new superconducting phase is under the pressure range of 3 GPa to 6 GPa. The high pressure Hall effect measurements indicated that the superconductivity caused by bulk hole pockets. The high pressure structure investigations with synchrotron X-ray diffraction indicated that the superconducting phase is of similar structure to that of ambient phase structure with only slight change with lattice parameter and internal atomic position. The topological band structures indicate the superconducting phase under high pressure remained topologically nontrivial. The results suggested that topological superconductivity can be realized in Bi_2Te_3 due to the proximity effect between superconducting bulk states and Dirac-type surface states. We also discussed the possibility that the bulk state could be a topological superconductor.

Keywords topological insulator, high pressure

PACS numbers 81.40.Vw, 03.65.Vf, 74.90.+n

Contents

1 Introduction

Topological insulators (TI) have generated great attentions in condensed matter physics recently [1–10]. TIs are materials which have a bulk band gap like an ordinary insulator, but have gapless surface states or edge states protected by time reversal symmetry on their boundaries [11, 12]. Dozens of materials are predicted as TIs [1, 6, 8, 13] and the number is still increasing, while several of them have been experimentally confirmed, such as HgTe/CdTe quantum well [3], $Bi_{1-x}Sb_x$ [4], Bi_2Se_3 [7], Bi_2Te_3 [5], Sb_2Te_3 [14], and $TlBiSe_2$ [10]. TIs have novel properties and potential applications, such as monopole like behavior [15] and topological magnetoelectric effect [16]. Particularly, on the interface of TI and superconductor, due to the superconducting proximity effect, Cooper pairs may tunnel from the superconductor to the surface, leading to an induced superconducting energy gap in the surface states that will create Majorana surface states [17]. Majorana fermions, half of ordinary Dirac fermions, can be very useful in quantum computing.

Topological superconductor, a cousin of TI, also have a full pairing gap in the bulk and gapless Majorana fermions states on the edge or surface [18–20]. However, the search for topological superconductors remains a challenge. Now from topological nontrivial band structure of TIs, superconductivity induced by doping in TIs

is a possible way to obtain topological superconductors. By copper intercalation doping in the van de Waals bond, Bi_2Se_3 turns to a superconductor with transition temperature T_c up to 3.8 K [21]. The superconductivity in $Cu_xBi_2Se_3$ occurs in bulk electron pockets separated from the surface states according to the ARPES results (Fig. 1) [22]. Three dimensional (3D) TIs doped into a superconducting phase are classified by an integer number n [19]. $Cu_xBi_2Se_3$ may be the first topological superconductor ever found if n is odd. Another possible topological superconductor is p type $TlBiTe_2$ which is a topological semi-metal for the normal state. The origin of superconductivity is caused by six leaflike hole pockets around the Γ point, similar to the ^{3}He–B phase which is considered to be topological fluid and contains Majorana fermions. However, the superconductivity in $TlBiTe_2$ needs further confirmation.

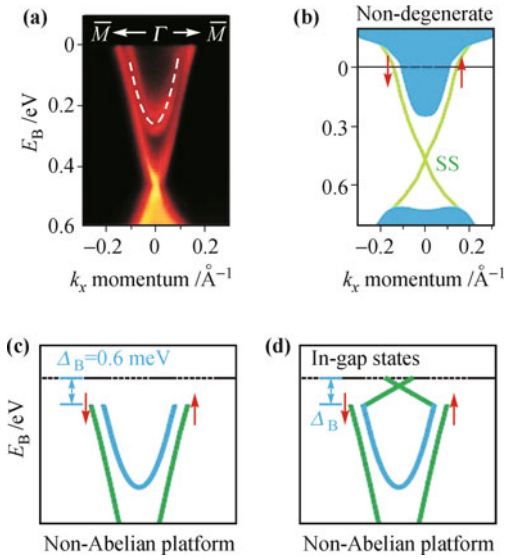

Fig. 1 **(a)** Momentum dependence of the bulk and surface conduction bands in superconducting $Cu_{0.12}Bi_2Se_3$ measured with low-energy (9.75 eV) photons for enhanced bulk sensitivity. **(b)** The surface electronic structure presents a non-trivial topological setting for superconductivity because (*green*) surface and (*blue*) bulk bands do not overlap. **(c)**, **(d)** Electronic states expected below T_c for even-parity superconductivity (c) and an example of odd-parity "topological superconductivity" (d).

High pressure is a powerful tool in tuning superconductivity by changing electronic structure. It is well documented that the record of high superconducting transition temperature T_c either for elements or compounds is created with the application of pressure. Moreover, high pressure can induce superconductivity in the matter that is not a superconductor at ambient pressure. Pressure tuning is almost free of introducing impurities or defects comparing with chemical substitution, so it is a superior way since it will be more intrinsic to mechanism studies. By applying high pressure on p type Bi_2Te_3, We found two superconducting phases between 3 GPa and 10 GPa before structure phase transition [23]. We studied the topological characters of two phases and compared them with superconducting $Cu_xBi_2Se_3$ and p-type $TlBiTe_2$. We further discussed the possibility of topological superconductivity.

2 Pressure induced superconductivity

Temperature dependence resistances at various pressures were performed to study the high pressure behaviors of Bi_2Te_3 (Fig. 2). A clear superconducting transition was observed at pressure above 3.2 GPa, with the transition temperature maintaining almost a constant up to 6.3 GPa. At higher pressure, a new superconducting phase appeared according to the resistance curves in Fig. 2(b). Contrasting with previous reports [24], we conjectured that the superconducting phase between 3.2 GPa and 6.3 GPa is a new superconducting phase while the phase above 6.3 GPa is consistent with that reported in Ref. [24], even though the transition temperature of the later phase is much higher than that in their report. The differences of the transition temperature may be caused by the carrier density. The data collected at 5.0 GPa showed that resistance dropped to zero at low

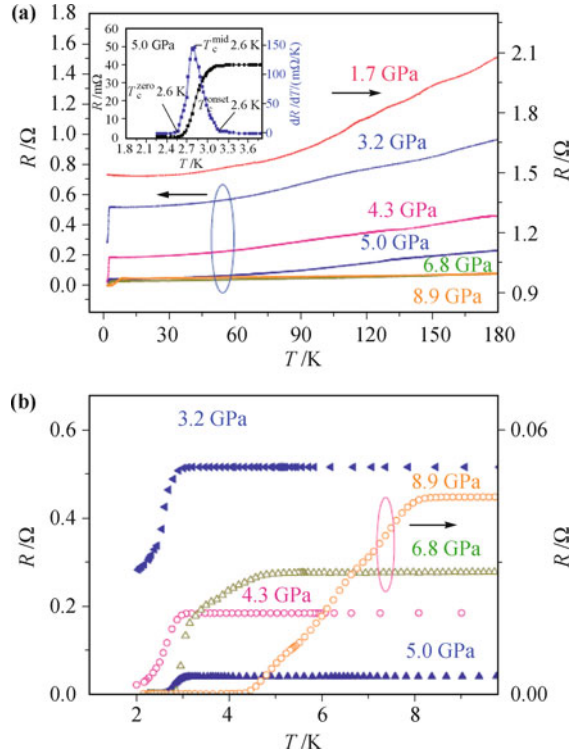

Fig. 2 **(a)** The resistances of Bi_2Te_3 single crystal as function of temperature at various pressures showing a superconducting transition around 3 K. The inset is the resistance near the critical temperature T_c with the differentiation of dR/dT showing the deffnition of T_c^{onset}, T_c^{mid} and T_c^{zero}, respectively; **(b)** The enlarged (low temperature) part of the measured resistance, indicatingrally different). A broad superconducting transition is observed for the intermediated pressure range, such as the data shown for 6.8 GPa the almost constant $T_c \sim 3$ K for the states between 3.1 GPa and 5.0 GPa, and a much higher T_c of 8.1 K at 8.9 GPa.

temperature, while the transition temperatures of onset, midpoint, or zero resistance were defined based on the differential of resistance over temperature (dR/dT) [inset of Fig. 2(a)]. The superconducting transition was sharp with the transition width (from 10% – 90% of the normal state resistance at T_c^{onset}) around 0.3 K, indicating the good homogeneity of the superconducting phase.

To assure that the transition in Fig. 2 is indeed a superconducting transition, we further conducted the electrical measurements around the transition temperature at variant external magnetic field. Figure 3(a) shows the measured resistance at 6.1 GPa with applied magnetic H. The transition temperature T_c decreased with increasing magnetic field H, indicating strong evidence that the transition is superconductivity in nature. The inset of Fig. 3(a) shows the change of T_c with applied magnetic field H. Using the Werthdamer–Helfand–Hohenberg formula of $H_{c2}(0) = -0.691[dH_{c2}(T)/dT]_{T=T_c} \cdot T_c$ [26], the upper critical field $H_{c2}(0)$ was extrapolated to be 1.8 Tesla for $H//c$, as the single crystal was placed inside the diamond anvil cell with magnetic field H direction perpendicular to ab-plane.

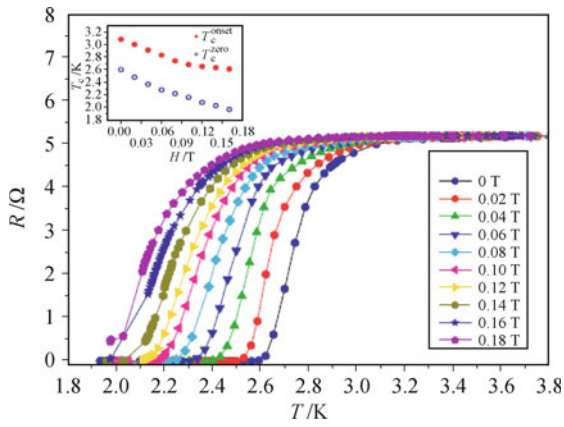

Fig. 3 The superconducting transition of Bi_2Te_3 single crystal at 6.1 GPa with applied magnetic field H perpendicular to the ab-plane of single crystal. Inset shows the change of T_c with H.

Carrier type and carrier density are important for superconductivity, and the earlier researches indicated that these two factors are also sensitive to the superconductivity of Bi_2Te_3 under pressure. The Hall effect measurements of Bi_2Te_3 at ambient pressure and high pressure are conducted to detect the carrier type and carrier density. The as grown single crystal is p type with the hole density approximately $(3 \sim 6) \times 10^{18}/cm^3$ at 2 K as calculated for several measurements at ambient pressure. Hall effect under high pressure is tested in a screw-type diamond anvil cell made of beryllium copper. Carrier density is calculated from the linear part of the Hall voltage under high field where the superconductivity has been destroyed already for the superconducting phase. Figure 4(a) shows the Hall voltage with the magnetic field at several fixed pressures and Fig. 4(b) shows the carrier density deduced from Fig. 4(a). The carrier density changes slightly in a fairly wide temperature range under fixed pressures. The carrier density at 4.3 GPa is about $6.2 \times 10^{18}/cm^3$ and changes smoothly with the increasing pressure below 5 GPa while suddenly jumped to a very high level more than $10^{23}/cm^3$ at the pressure around 6 GPa. The results are similar to those reported in Ref. [25]. As the density of the free electron in good metal is of the order $10^{22}/cm^3$, we inferred that the carrier density calculated from Hall effect is unreasonable. Since there is no structure phase transition or isostructure phase transition around 6 GPa, we do not expect the dramatic change of the carrier mobility. As the resistivity around that pressure has no dramatic change, we can also infer that the sudden change of the carrier density is not true. One reasonable explanation is that the material turns into a semi-metal in which the conduction electron and hole pockets coexist. Since the Hall voltages caused by the electrons and that by holes have opposite sign and can mutually counteract, the carrier density cannot be calculated by Hall effect any more. This deduction can also explain the sudden drop of the thermoelectrical power above 6 GPa [27]. Refer to the change of the pressure dependence resistivity, we deduced that the superconductivity in our experiments is caused by hole

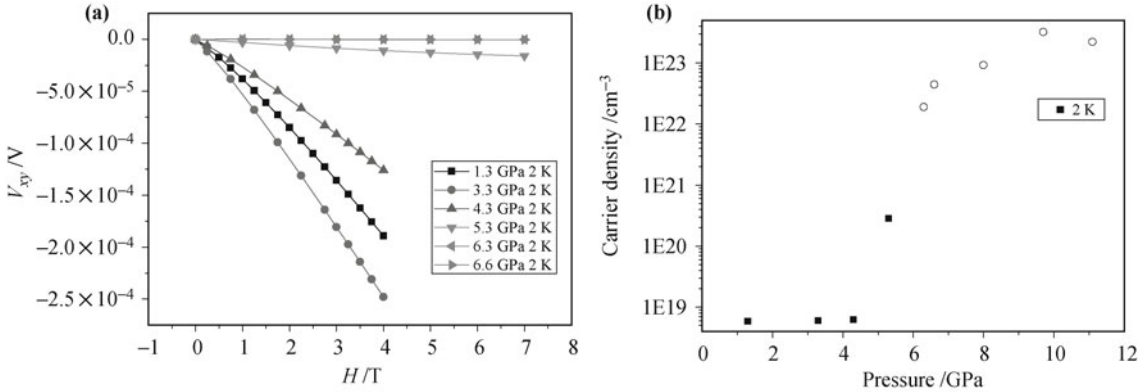

Fig. 4 **(a)** The Hall voltage of Bi_2Te_3 single crystal with magnetic field H perpendicular to the ab-plane of the single crystal. **(b)** The carrier density deduced from the linear part of Hall resistance at various pressure at 2 K. The circles indicate the carrier density data is unreasonable.

carriers with the carrier density in the range of $10^{18}/cm^3$ to $10^{20}/cm^3$ for both two superconducting phases. More tests on samples with different carrier type and different carrier density should be conducted to verify the effect to the superconductivity, however, the hole density has little effect to the topological characters according to the theoretical calculation which will be discussed later.

To check whether the superconducting phase under high pressure is caused by structure phase transition, we conducted synchrotron X-ray diffraction experiments with pressure from ambient to above 30 GPa in an average 2 GPa step at room temperature. Figure 5 shows the high pressure X-ray diffraction patterns of Bi_2Te_3 polycrystalline (ground from the single crystal) at several selected pressure levels. The patterns show that the ambient phase remained stable up to 6.3 GPa. A new set of peaks not belong to ambient structure phase appear in the pattern of 8.6 GPa, which indicates there is a structure phase transition in the range of 6.3 GPa to 8.6 GPa. These results are consistent with previous reports that the structure phase transition occurs at 8 GPa [24, 30]. Low temperature X-ray diffraction at 8K was performed to confirm the structure phase transition pressure at the temperature when the superconducting occurs. The lattice parameters calculated by unit cell at 8 K are almost the same with that at room temperature, which shows the thermal expansion coefficient is very little. The room temperature X-ray diffraction patterns under high pressure are refined using Rietveld method with GSAS package.

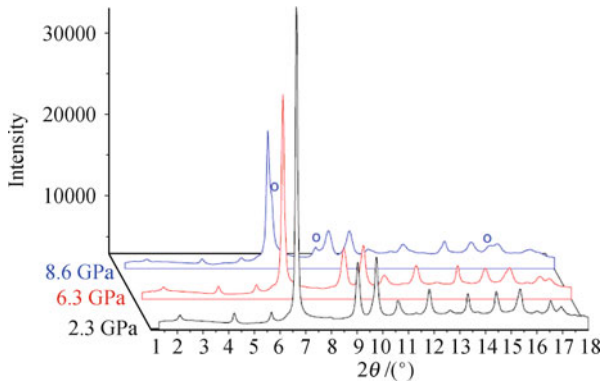

Fig. 5 The synchrotron X-ray diffraction patterns of Bi_2Te_3 samples at selected pressures showing the ambient structure is stable at least up to 6.3 GPa, and a structurally deferent phase appears at 8.6 GPa (the circle indicating the peaks from new structure).

3 The topological characters under high pressure

3.1 Topological band structure

The topological property of Bi_2Te_3 has been theoretically predicted from first-principle calculations and analytical models [6] and is confirmed by the Angle Resolved Photon Electron Spectroscopy (ARPES) measurement of surface states [5, 14]. Due to the strong spin–orbit coupling, the band structures around the Γ point of the Brillouin zone (BZ) are inverted, similar to the case of HgTe quantum wells [1], which gives rise to the TI behavior. As the superconducting phase of Bi_2Te_3 under high pressure has similar structure to the ambient phase with small changes of lattice parameters and atomic positions, we can conjecture the topological band structure. Directly probing the surface states or topological characters is difficult, however, first-principle calculations are proved to be an effective mean in predicting TIs. The band structures and surface states of TIs obtained by first principle calculations can be well compared with the ARPES measurement [5, 6]. It is reasonable for us to believe that the band structures and surface states under pressure can be well simulated by first principle calculations as well as under ambient pressure.

Using the first-principles calculations based on density functional theory and the generalized gradient approximation, we performed full relativistic electronic structure calculations for Bi_2Te_3 at both 0 and 4 GPa, using the experimental lattice parameters and atomic positions obtained from the X-ray refinements. For the calculations of surface states, we used a thick slab consisting of 40 QLs. For the 0 GPa phase, our calculations well reproduced those found in earlier results [9, 14] [Figs. 6(a) and (b)]. In particular, the calculated surface states can be well compared with the ARPES measurement [5, 14]. Although the electronic structure at 4 GPa was quite similar to that at 0 GPa, the electronic structures at 4 GPa were, in fact, quantitatively different with that of 0 GPa [Figs. 6(c) and (d)]. The differences are as follows: (i) the direct gap at Γ point is enhanced while the indirect bulk band gap is reduced and (ii) the separation between surface states and bulk states at the Fermi level is further enhanced. Most importantly, by calculating the Z_2 number from parity analysis and the surface states, we confirmed that the compound remained topologically nontrivial at 4 GPa. We also relaxed the lattice constants and internal atomic sites theoretically for both cases and confirmed that all features of the electronic structures discussed here did not change.

For the second superconducting phase at the pressure range between 6 GPa and 10 GPa. Refer to the wind of the changes under pressure mentioned above, the indirect gap decreased with the increasing pressure and became zero at a critical pressure P_c. For higher pressure, the indirect gap becomes negative. If the direct gap remains, the band structure can transform to that of ambient pressure through smooth adiabatic changes, therefore both the two superconducting phases have the same topological class. Moreover, the semi-metal band structure of the second superconducting phase is very similar to that of the p type $TlBiTe_2$ which was verified to be a

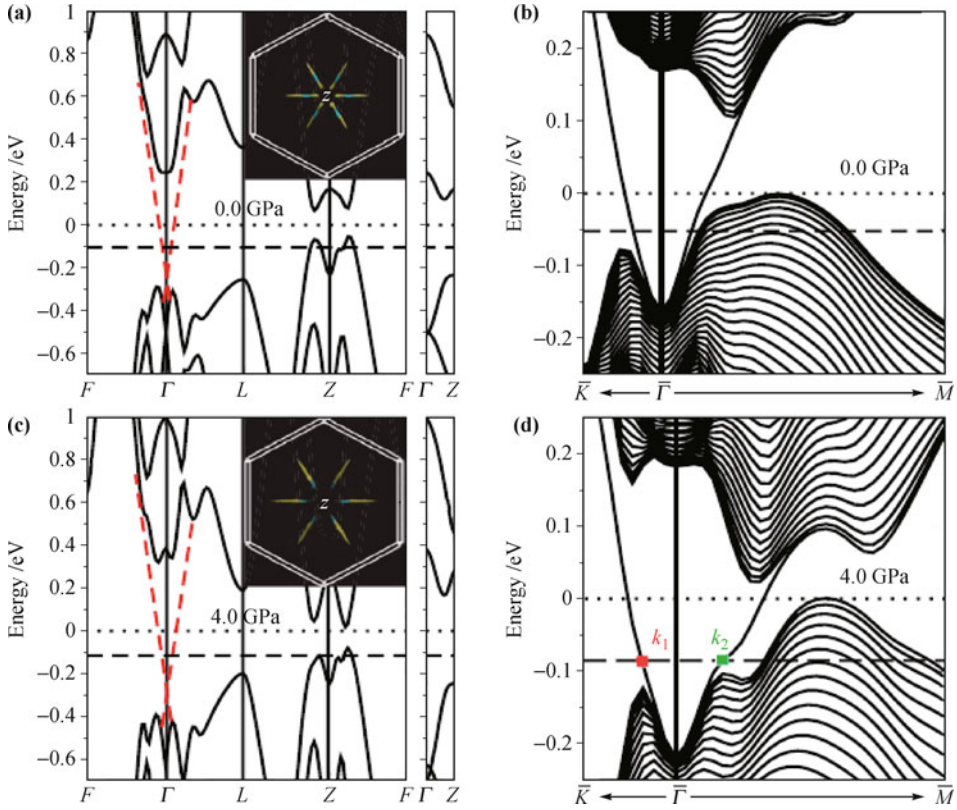

Fig. 6 The calculated bulk electronic structures (*left panels*) and surface states (*right panels*) of the Bi_2Te_3 at 0.0 GPa [**(a)** and **(b)**] and 4.0 GPa [**(c)** and **(d)**], respectively. The chemical potential corresponding to the experimental hole concentration ($5.8 \times 10^{18}/cm^3$) are indicated as horizontal dashed lines and the corresponding Fermi surfaces are also shown as insets. In order to understand the k-space separation of bulk and surface states, we show the surface states schematically in the bulk band structures (*left panels*).

topological semi-metal. However, the topological properties of the second conducting phase needs to be further confirmed.

3.2 Superconducting proximity effect

Now we focus on the bulk-to-surface proximity effect, two critical criteria should be satisfied which were discussed at the beginning. Luckily, Bi_2Te_3 has the particular property, in which the surface states are located around the Γ point, while both conduction band minimum (CBM) and valence band maximum of bulk states are located away from the Γ point. In other words, for the low energy range, the surface states and bulk states were well separated in the momentum space (Fig. 6). The direct band gap at Γ point was much bigger than the indirect bulk band gap, which was formed from states around the Z point of the bulk BZ. In contrast to Bi_2Te_3, for the electron-doped Bi_2Se_3, the CBM of bulk states were located around the Γ point, very close to the surface states. For the phase under 4 GPa, direct gap at Γ point and separation of surface states between bulk states at the Fermi level is enhanced as mentioned before. For the superconducting phase of Bi_2Te_3 under pressure, we have also analyzed the penetration depth of surface states around the Fermi energy as determined by the experiments [k_1 and k_2 points shown in Fig. 6(d)]. We found that the surface states were exponentially localized to the surface region with half-widths of about 3 QLs. Using the rigid band model, we further estimated the Fermi level position as functions of carrier concentration and found that the surface states remained to be well defined even if the carrier density was as high as $10^{21}/cm^3$ (hole type). For our experimental situation, where superconductivity was observed, the carrier density (of the order of $10^{18}/cm^3$) was much smaller than this level for the superconducting phase under 4 GPa. Both facts support our conclusion that the topological surface states can maintain their character in the presence of the p-type bulk carriers. Therefore, the resulting proximity effect with the bulk superconducting carriers can give rise to Majorana fermions in the surface state.

For the second superconducting phase, the semimetal band structure is similar to the superconducting $TlBiTe_2$, and the superconductivity also comes from the hole pockets. Since both conduction band minimum and valence band maximum of bulk states are away from Γ point, the surface states may remain well separated from the bulk. However, more researches should be performed to verify its topological class.

3.3 Possibility of topological superconductivity

We now turn to the exciting possibility that the bulk superconducting state in Bi_2Te_3 could be a topological superconductor [8, 13, 18–20, 31, 32]. In insets of Figs. 6(a) and (c), we see that with p type doping, holes form disconnected pockets. Pairing amplitude on a given hole pocket could be largely determined by the phonon contribution mediated at the small momentum transfer, and a uniform pairing order parameter could be established on each hole pocket. The relative pairing amplitude among the different hole pockets would be determined by the large momentum transfer, where the Coulomb repulsion plays a more dominant role. Such a repulsive interaction generally favors opposite pairing amplitudes on different Fermi pockets, leading to a negative Josephson coupling among the neighboring hole pockets. However, due to the three-fold symmetry of the Fermi surface, such a coupling is frustrated, so that the pairing order parameter in the ground state may become complex. A natural choice of such a complex orbital pairing symmetry without breaking the time reversal symmetry is a triplet pairing symmetry similar to the BW state in ^{3}He-B phase. Such a pairing state has been shown on general grounds to be a topological superconducting state respecting the time reversal symmetry.

4 Summary

In summary, we have experimentally observed superconductivity in Bi_2Te_3 under pressure, where the crystal structure remains the same as the ambient topological phase. Topological surface states remain to be well defined under pressure, and in the presence of bulk p type carriers, and this natural bulk-surface proximity effect could give rise to Majorana fermions on the surface. We also discussed the pairing symmetry of the bulk superconducting state, and addressed the possibility that it could realize the 3D topological superconductor with time reversal symmetry.

5 Methods

The superconducting measurements induced via high pressure were conducted by using diamond anvil cell technique as described in Ref. [33]. The diamond culet is 300 μm in diameter. A plate of T301 stainless steel covered with MgO fine powders in order to protect the electrodes leads from short circuit was used as gasket. The gasket, preindented from the thickness of 300 μm to 60 μm, was drilled a hole of 180 μm diameter where MgO fine powders were pressed. The pressed MgO was further drilled into a small hole of 100 μm diameter to serve as sample chamber wherein a Bi_2Te_3 single crystal with the dimension of 60 μm×30 μm×10 μm was inserted into the center with soft hBN fine powder as pressure transmitting medium that can provide a good hydrostatic pressure environment. A small ruby was put aside the specimen. Pressure was measured by using ruby florescent method [34, 35]. We use slim Au wire of 10 μm diameter as electrodes. Four-probe method was adapted to measure the resistivity. A screw type diamond anvil cell made of BeCu was used to conduct low temperature experiments. The diamond anvil cell was put inside a Mag Lab system upon loading. The temperature was automatically program controlled via the Mag Lab system. We specially mounted a thermometer around the sample in the diamond anvil cell to monitor the sample temperature. The data are collected at each equilibrium point of temperature. The high pressure Hall effects are measured based on Van der Pauw method using a piston cylinder type instrument that is inserted into the Mag Lab system.

The X-ray diffraction experiments at high pressure with synchrotron radiation are done at HPCAT of Advanced Photon Source (APS) of Argonne National Lab (ANL) with wavelength 0.368 Å using a symmetric Mao Bell diamond anvil cell at room temperature. The crystal structures are refined using GSAS package.

We calculate the electronic structures of Bi_2Te_3 with their experimental crystal structures (for 0.0 GPa and 4.0 GPa), respectively. The first-principles calculations are performed using OpenMX package [36], which is based on a linear combination of pseudo-atomic orbital (PAO) method. The PAOs are generated by a confinement potential scheme with a cutoff radius of 9.0 and 7.5 a. u. for Bi and Te, respectively. Basis set with s2p2d2f1 PAOs for Bi and s2p2d3 for Te is found to be good enough to describe our system. The exchange correlation energy functional within generalized gradient approximation as parameterized by Perdew, Burke and Ernzerhof is used. Brillouin zone is sampled with 10×10×4 grids. We construct the projected atomic Wannier (PAW) functions [9] for s and p orbitals of both Bi and Te. With this set of PAW bases, an effective model Hamiltonian for slab of 40 QLs is established and the topologically nontrivial surface state can be obtained from it.

Acknowledgements We acknowledge the financial support from the National Natural Science Foundation of China and Ministry of Science and Technology of China (Grant Nos. 2009CB929402, 10820101049, and 90921005).

References and notes

1. B. A. Bernevig, T. L. Hughes, and S. C. Zhang, Science, 2006, 314(5806): 1757
2. L. Fu and C. L. Kane, Phys. Rev. B, 2007, 76(4): 045302
3. M. König, S. Wiedmann, C. Brüne, A. Roth, H. Buhmann,

L. W. Molenkamp, X. L. Qi, and S. C. Zhang, Science, 2007, 318(5851): 766

4. D. Hsieh, D. Qian, L. Wray, Y. Xia, Y. S. Hor, R. J. Cava, and M. Z. Hasan, Nature, 2008, 452: 970
5. Y. L. Chen, J. G. Analytis, J. H. Chu, Z. K. Liu, S. K. Mo, X. L. Qi, H. J. Zhang, D. H. Lu, X. Dai, Z. Fang, S. C. Zhang, I. R. Fisher, Z. Hussain, and Z. X. Shen, Science, 2009, 325(5937): 178
6. H. J. Zhang, C. X. Liu, X. L. Qi, X. Dai, Z. Fang, and S. C. Zhang, Nat. Phys., 2009, 5: 438
7. Y. Xia, D. Qian, D. Hsieh, L. Wray, A. Pal, H. Lin, A. Bansil, D. Grauer, Y. S. Hor, R. J. Cava, and M. Z. Hasan, Nat. Phys., 2009, 5 : 398
8. J. C. Y. Teo, L. Fu, and C. L. Kane, Phys. Rev. B, 2008, 78(4): 045426
9. W. Zhang, R. Yu, H. J. Zhang, X. Dai, and Z. Fang, New J. Phys., 2010, 12: 065013
10. Y. L. Chen, Z. K. Liu J. G. Analytis, J. H. Chu, H. J. Zhang, B. H. Yan, S. K. Mo, R. G. Moore, D. H. Lu, I. R. Fisher, S. C. Zhang, Z. Hussain, and Z. X. Shen, Phys. Rev. Lett., 2010, 105(26): 266401
11. X. L. Qi and S. C. Zhang, arXiv:1008.2026v1, 2010
12. M. Z. Hasan and C. L. Kane, Rev. Mod. Phys., 2010, 82(4): 3045
13. B. H. Yan, C. X. Liu, H. J. Zhang, C. Y.Yam, X. L. Qi, T. Frauenheim, and S. C. Zhang, Europhys. Lett., 2010, 90(3): 37002
14. D. Hsieh, Y. Xia, D. Qian, L. Wray, F. Meier, J. H. Dil, J. Osterwalder, L. Patthey, A. V. Fedorov, H. Lin, A. Bansil, D. Grauer, Y. S. Hor, R. J. Cava, and M. Z. Hasan, Phys. Rev. Lett., 2009, 103(14) : 146401
15. X. L. Qi, R. D. Li, J. D. Zang, and S. C. Zhang, Science, 2009, 323(5918) : 1184
16. X. L. Qi, T. L. Hughes, and S. C. Zhang, Phys. Rev. B, 2008, 78(19): 195424
17. L. Fu and C. L. Kane, Phys. Rev. Lett., 2008, 100(9): 096407
18. X. L. Qi, T. L. Hughes, S. Raghu, and S. C. Zhang, Phys. Rev. Lett., 2009, 102(18): 187001
19. A. P. Schnyder, S. Ryu, A. Furusaki, and A. W. W. Ludwig, Phys. Rev. B, 2008, 78(19): 195125
20. S. Ryu, A. P. Schnyder, A. Furusaki, and A. W. W. Ludwig, New J. Phys., 2010, 12: 065010
21. Y. S. Hor, A. J. Williams, J. G. Checkelsky, P. Roushan, J. Seo, Q. Xu, H. W. Zandbergen, A. Yazdani, N. P. Ong, and R. J. Cava, Phys. Rev. Lett., 2010, 104(5): 057001
22. L. A. Wray, S. Y. Xu, Y. Xia, Y. S. Hor, D. Qian, A. V. Fedorov, H. Lin, A. Bansil, R. J. Cava, and M. Z. Hasan, Nat. Phys., 2010, 6: 855
23. J. L. Zhang, S. J. Zhang, H. M. Weng, W. Zhang, L. X. Yang, Q. Q. Liu, S. M. Feng, X. C. Wang, R. C. Yu, L. Z. Cao, L. Wang, W. G. Yang, H. Z. Liu, W. Y. Zhao, S. C. Zhang, X. Dai, Z. Fang, and C. Q. Jin, Proc. Natl. Acad. Sci. USA, 2011, 108(1): 24
24. M. Einaga, Y. Tanabe, A. Nakayama, A. Ohmura, F. Ishikawa, and Y. Yamada, J. Phys.: Confer. Ser., 2010, 215(1): 012036
25. C. Zhang et al., Phys. Rev. B, 2011,
26. N. R. Werthamer, E. Helfand, and P. C. Hohenberg, Phys. Rev., 1966, 147: 295
27. S. V. Ovsyannikov, V. V. Shchennikov, G. V. Vorontsov, A. Y. Manakov, A. Y. Likhacheva, and V. A. Kulbachinskii, J. Appl. Phys., 2008, 104 : 053713
28. A. Nakayama, M. Einaga, Y. Tanabe, S. Nakano, F. Ishikawa, and Y. Yamada, High Pressure Research, 2009, 29 : 245
29. M. Einaga, A. Ohmura, A. Nakayama, F. Ishikawa, Y. Yamada, and S. Nakano, Phys. Rev. B, 2011, 83(9): 092102
30. B. H. Toby, Journal of Applied Crystallography, 2001, 34: 210
31. X. L. Qi, T. L. Hughes, and S. C. Zhang, Phys. Rev. B, 2010, 81(13): 134508
32. L. Fu and E. Berg, Phys. Rev. Lett., 2010, 105(9): 097001
33. H. K. Mao and P. M. Bell, Science, 1976, 191(4229): 851
34. S. J. Zhang, X. C. Wang, R. Sammynaiken, J. S. Tse, L. X. Yang, Z. Li, Q. Q. Liu, S. Desgreniers, Y. Yao, H. Z. Liu, and C. Q. Jin, Phys. Rev. B, 2009, 80(1): 014506
35. S. J. Zhang, X. C. Wang, Q. Q. Liu, Y. X. Lv, X. H. Yu, Z. J. Lin, Y. S. Zhao, L. Wang, Y. Ding, H. K. Mao, and C. Q. Jin, Europhys. Lett., 2009, 88(4): 47008
36. http://www.openmx-square.org/